Apical Four-Chamber Echocardiography Segmentation using Marker-controlled Watershed Segmentation

Nonthaporn Nakphu, Dyah Ekashanti Octorina Dewi, Muhammad Qurhanul Rizqie, Eko Supriyanto, Ahmad 'Athif Mohd Faudzi, Dolwin Ching Ching Kho, Suhaini Kadiman, and Panrasee Rittipravat

***Abstract*— Echocardiography provides information about size, shape, and function of heart to create the image. Apical four-chamber echocardiography can be obtained by placing the ultrasound probe at the apex of the left ventricle. Such view enables to analyze heart abnormalities. In this regard, chamber quantification is recommended to evaluate the heart volume by defining the endocardial border of the chambers. Image segmentation that subdivides an image into different regions may be suitable to analyze the chambers. In this study, we propose a Marker-controlled Watershed segmentation method. It involves Watershed Transform, internal and external markers, and morphological processing. The advantage is that it can control over-segmentation due to noise and other local irregularities. We tested the proposed method on an apical four-chamber echocardiography image and a model image. We also compared the segmentation result with an Active Contour-based segmentation method. The results show that the Watershed Transform performs better than Active Contour.**

I. Introduction

Echocardiography uses two-, three-dimensional static image, and a moving image of heart. It provides important information, such as size and shape of the heart as well as heart chambers, pumping capacity, and the location of tissue damage. It is used for diagnosing and following-up treatment of the patients with suspected or known heart diseases.

N. Nakphu is undergraduate student of the Department of Biomedical Engineering, Faculty of Engineering, Mahidol University, Salaya, Nakorn Pathom 73170 Thailand (e-mail: nonthaporn.nak@student.mahidol.ac.th).

D. E. O. Dewi is with the IJN-UTM Cardiovascular Engineering Center, University Technology Malaysia, Skudai, Johor 81310 Malaysia (e-mail: dyah.ekashanti@gmail.com).

M. Q. Rizqie is with IJN-UTM Cardiovascular Engineering Centre, Faculty of Biosciences and Medical Engineering, Universiti Teknologi Malaysia, and Faculty of Computer Science, Universitas Sriwijaya, Indonesia (e-mail: qurhanhul.rizqie@gmail.com).

E. Supriyanto is with the IJN-UTM Cardiovascular Engineering Center, University Technology Malaysia, Skudai, Johor 81310 Malaysia (e-mail: eko@biomedical.utm.my).

A. A. Mohd Faudzi is with IJN-UTM Cardiovascular Engineering Center, Control and Mechatronics Engineering Department-Faculty of Electrical Engineering, and Centre for Artificial Intelligent and Robotics, University Technology Malaysia, Skudai, Johor 81310 Malaysia (e-mail: athif@fke.utm.my)

D. C. C. Kho is with the IJN-UTM Cardiovascular Engineering Center, University Technology Malaysia, Skudai, Johor 81310 Malaysia (e-mail: kccdolwin2@live.utm.my).

S. Kadiman is with the National Heart Institute, Kuala Lumpur 50400 Malaysia (e-mail: suhaini@ijn.com.my).

P. Rittipravat is with the AIM LAB, Department of Biomedical Engineering, Faculty of Engineering, Mahidol University, Salaya, Nakorn Pathom 73170 Thailand (e-mail: panrasee.rit@ mahidol.ac.th).

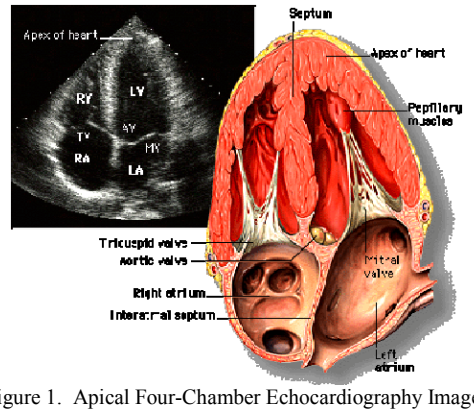

Figure 1. Apical Four-Chamber Echocardiography Image. (*Source : http:// www.yale.edu/imaging/echo_atlas /views/graphics/ 4_chamber.gif*)

Transthoracic echocardiography is the most commonly performed echocardiography. The images are obtained from at least four different probe positions with different details of the heart. The standard positions are parasternal, apical, subcostal, and suprasternal notch positions. The apical four-chamber view is one of the views that the apical position can acquire. This view, as given in Fig, 1, can be obtained by placing the probe at apex of the left ventricle or the point at maximal impulse and orienting the probe towards the right shoulder. It displays four chambers of the heart; right ventricle, left ventricle, right atrium, left atrium, mitral valve, tricuspid valve, inter-ventricular, and inter-atrial septa [1]-[3]. This view detects congenital heart disease, measures right and left ventricular capacity, ejection fraction, and analyzes wall-motion in adults [4],[5],[6] and fetuses [8],[9], but not much in pediatrics [4],[7]. For these purposes, chamber quantification is recommended to analyze the chamber volume by defining the endocardial border. The analysis methods for apical four-chamber echocardiography image can be classified into manual and automatic. For automatic methods, some involves image enhancement, image segmentation, and texture analysis.

Image segmentation has been widely used in computer-based echocardiography analysis, such as, finding the capacity of left and right ventricles [12], thickness of left ventricular wall [13], and characterizing tissues [14]. Image segmentation usually employs edge detection, thresholding, morphology or Watershed segmentation, and region-oriented approaches. There are three methods that have been applied using Watershed segmentation; distance transform, gradients, and marker-controlled improved from gradient image [12].

978-1-4799-4084-4/14/$31.00 ©2014 IEEE

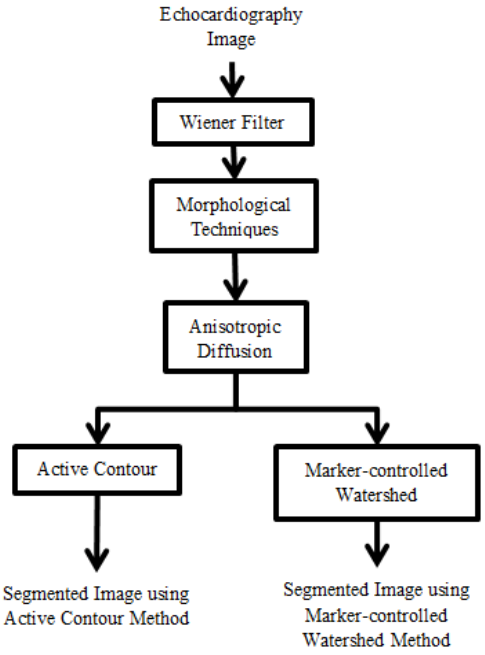

Figure 2. Block Diagram of the Study.

In this study, we segmented the apical four-chamber view region of normal adult echocardiography image using Marker-controlled Watershed (McW). We compared the segmented image between the proposed and Active Contour (AC) method. Block diagram of this study is shown in Fig.2. In Chapter I, we explain about the introduction of the study. Chapter II describes materials and methods that we used in image segmentation. Chapter III presents the results and discussion. The conclusion and future research direction is given in Chapter IV.

II. Materials and Methods

In this study we explored two methods for apical four-chamber echocardiography image segmentation; active contour and marker-controlled watershed methods.

A. Wiener Filter (WF)

We employed a two-dimensional adaptive noise removal WF for pre-processing. It uses a pixel-wise adaptive Wiener method based on statistics estimated from a local neighborhood of each pixel. We must determine the appropriate size of neighborhoods to estimate the local image mean and standard deviation [15].

B. Morphological Techniques

Mathematical morphology extracts image components for representation and description of region shapes. There is a structuring element (SE), a shape to probe or interact with the image to fit the shape. SE is used in morphological operations, such as dilation, erosion, opening, and closing. There are two characteristics that are related to it, shape and size, depending on the image content.

We used *Opening-by-reconstruction* followed by *Closing-by-reconstruction* for pre-processing and cleaning up binary image. These are morphological reconstructions that involve two images and an SE. Two images are marker as the starting point for the transformation, and mask that constrains the transformation. *Opening-by-reconstruction* restores exactly the shapes of the objects that remain after erosion. The eroded image is used as the marker image in a reconstruction. The original image is used as the mask. *Closing-by-reconstruction* is done by complementing an image, computing its *Opening-by-reconstruction*, then complementing the result. [11]

C. Anisotropic Diffusion (AD)

Anisotropic diffusion filter is Partial Different Equation (PDE)-based technique for smoothing and restoration purposes. We used the modified code from [16] that employed the Perona-Malik (PM) equation. PM model uses nonlinear diffusion and does edge enhancement. It applies inhomogeneous process that reduces the diffusivity at those locations with larger likelihood to be edges. This likelihood is measured by $|\nabla u|^2$. The PM filter [19] is given as follows

$$\partial_t u = \operatorname{div}\left(g(|\nabla u|^2)\ \nabla u\right). \qquad (1)$$

D. Active Contour (AC)

The AC models or snakes can evolve a curve to detect the boundary of objects in the image based on gradient. We used the modified code from [17] by Chan and Vese [20] for image segmentation. This model is based on curve evolution technique, Mumford-Shah function for segmentation and level sets. They minimize an energy which can be seen as a particular case of the minimal partition problem. The characteristics of this code are initial curve and iterations.

E. Marker-controlled Watershed Segmentation (McW)

The McW is based on marker and working as over-segmentation controller. The Watershed Transform (WT) solves a variety of image segmentation problems. If there are two drops of water near each other, the WT finds the catchment basins and ridge line in a gray-scale image. McW used internal markers, inside each of the region of interest, and external markers, background of image, to modify the gradient image. Various methods have been used for computing internal and external markers which involve in the linear filtering, nonlinear filter, and morphological operation. In this study, we used morphological operation to calculate internal and external markers. The characteristic of the McW method is the region minima. [12]

III. Results and Discussion

Our experiments consist of several parts, ranging from testing the segmentation algorithm using dummy image, manually drawn model image, to the apical four-chamber echocardiography image.

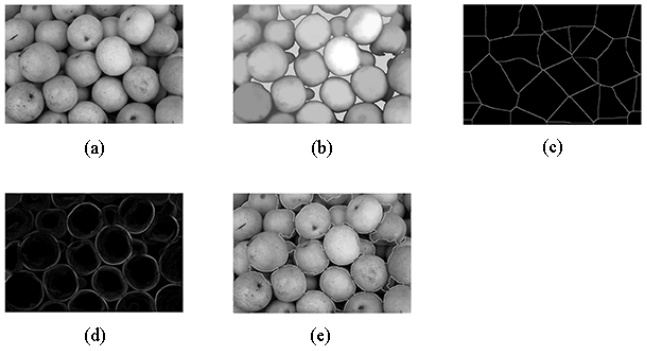

Figure 3. McW method [12] on dummy image (a) Original image from http://www.mathworks.com/help/images/examples /WatershedSegmentationExample_01.png (b) Internal marker (c) External marker (d) Modified gradient magnitude (e) Segmented image

The proposed methods were encoded using MATLAB 7.8.0 (R2009a) and some of technique codes employed Image Processing Toolbox in MATLAB. The performance of the methods was tested by using MeTriX MuX [18].

The dummy image in Fig. 3(a) shows an example of McW segmentation method [12]. We applied morphological operation and some pre-processing on the image. Then, we computed the WT of the gradient image and used extended-minima transform to obtain the set of internal marker as shown in Fig. 3(b). The external marker (Fig. 3(c)) is obtained by computing the WT of the distance transform of internal marker image. We used internal and external marker images to modify the gradient image by using the intensity image from morphological reconstruction resulting Fig. 3(d). Fig. 3(e) gives the segmentation result by showing the Watershed ridgelines computed from the WT of the marker-modified gradient image.

The manually drawn model image in Fig. 4(a) is meant to quantitatively measure the performance of the pre-processing and McW methods by calculating the image quality between original and noised images after the segmentation. We added the speckle noise (variance = 0.50) in Fig. 4(b). The WF image, as shown in Fig. 4(c), could not remove the noise properly. Therefore, we needed to apply morphological reconstruction, and worked properly in cleaning up the image (Fig. 4(d)). The segmented model image by McW is given in Fig. 4(f).

It can be seen that the whole region of interest can be segmented by using the parameters of pre-processing and McW methods. In comparison between the segmented model image and speckle noise of the model image by using pre-processing and McW methods, it can be seen that both are perfectly segmented. However, the segmented region surface of segmented speckle noise model image (Fig. 4(a)) is different from the one of segmented original model image (Fig. 4(f)). The quantitative measurement of image quality of the model image is computed by MeTriX MuX and given in Table I.

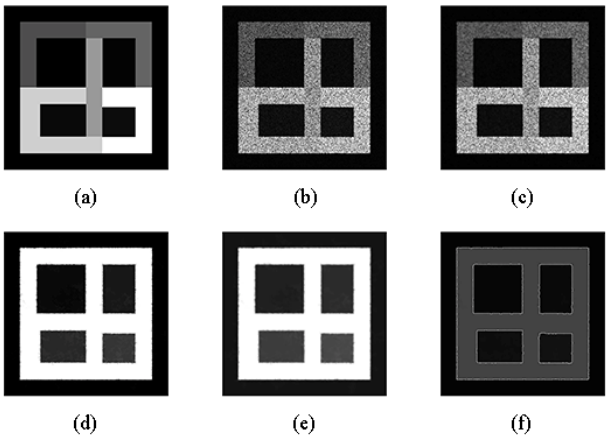

Figure 4. Manually drawn model image with speckle noises tested for image segmentation using Marker-Controlled Watershed Segmentation Method. (a) Original Model Image. (b) Speckle Noise Model Image (variance=0.50). (c) WF Image (neighborhoods of size 5-by-5). (d) Opening- and Closing-by-Reconstruction Filtered Image (structure shape=diamond, size=20). (e) AD Filtered Image (iteration=5, kappa=30). (f) Segmented Image by McW Method (region minima=3).

TABLE I. IMAGE QUALITY ASSESSMENT OF SEGMENTED MODEL IMAGE

Image Quality Assessment	Value
MSE	5776.190254
PSNR	10.514389
SSIM	0.790298
MSSIM	0.691217
VSNR	16.099332
VIF	0.121483
VIFP	0.155188
UQI	0.460006
IFC	0.842111
NQM	5.978685
WSNR	4.22826
SNR	3.508199

Fig. 5 gives the image segmentation results of the apical four-chamber echocardiography image. Fig. 5(a) is the original one. Fig. 5(b) shows a good result after using WT. Some of the noise can be removed from the original image. Morphological techniques, opening- by-reconstruction followed by closing-by-reconstruction were done afterwards. Fig. 5(c) also shows good result to clean up the image after WT. We applied AD filter in Fig. 5(c) and the filtered image, as presented in Fig. 5(d), gives smooth result while the edge is still enhanced as expected. Fig. 5(e) is the segmented image result of AC method. The region of heart wall cannot be segmented perfectly. In Fig. 5(f), the mask of the segmented image shows the region the right atrial chamber was the only heart chambers that this method could segment.

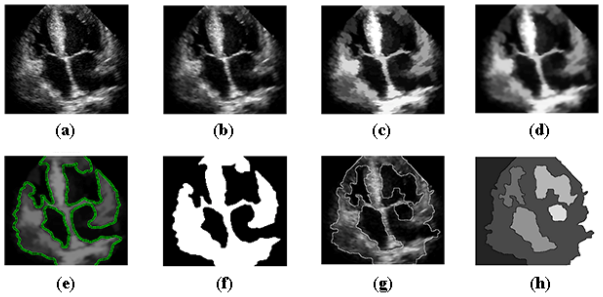

Figure 5. Apical Four-Chamber echocardiography image tested for image segmentation. (a) Cropped Apical Four-Chamber Original Image taken from *(http://fas.org /irp/imint/docs/rst/Intro/apical_four_chamber_view.jpg)* (b) WF Image. (c) Opening- and Closing-by-Reconstruction Filtered Image. (d) Anisotropic Diffusion Filtered Image. (e) Segmented Image by AC Method. (f) Mask of Segmented Image (e). (g) Segmented Image by Mcw Method. (h) Marker of Segmented Image (g).

In Fig. 5(g), as the result of McW method, the left atrial chamber was the only heart chamber that has incomplete segmented region. While in Fig. 5(h), the regions of each part are segmented properly. However, the constraint is that if we change the parameters, the result can be different. For AC method, the region of heart wall could be segmented better, but could not cover the whole heart wall. It also included the region of the heart chamber. The result after using McW method in different parameter could be also over-segmentation.

IV. Conclusion and Future Research Direction

From our experiment on apical four-chamber echocardiography image segmentation, we can conclude that Marker-controlled Watershed (McW) segmentation method has better segmentation than Active Contour (AC) method. Pre-processing and filtering parameters have effects on segmentation. We also found that the most effective pre-processing method for our case is morphological technique.

For the future direction, we will improve this apical four-chamber echocardiography image segmentation study for tissue characterization, three-dimensional ultrasound reconstruction and analysis, as well as image fusion of ultrasound and CT of the heart.

Acknowledgment

The authors would also like to thank IJN-UTM Cardiovascular Engineering Center for research and collaboration in industrial internship from Department of Biomedical Engineering, Faculty of Engineering, Mahidol University, Thailand, for the period of 1 April 2014 to 30 June 2014.

This research and publication is made possible with the supports from Flagship Grant of '3D Position Tracking for Image Fusion of CT and ultrasound images of the heart' (Q.J130000.2409.01G90) and Flagship Grant of 'Development of Transesophageal Echocardiography (TEE) Probe Remote Positioning Control Unit' (Q.J130000.2409.01G69).

The authors would also acknowledge Universiti Teknologi Malaysia and Ministry of Education, Malaysia, for all supports.

References

[1] A. Qasim and A. Raina. *Transthoracic Echo* [online]. Available: http://echocardiographer.org/TTE.html.

[2] D. Mereles. *Transthoracic examination* [online]. Available: http://www.echobasics.de/tte-en.html.

[3] Stanford University. *4 chamber view* [online]. Available: https:// web.stanford.edu/group/ccm_echocardio/cgi-bin/mediawiki /index.php/4_chamber_view.

[4] F. Ichida et al, "Cardiac chamber growth pattern determined by two-dimensional echocardiography," *Heart Vessles*, vol. 4, pp. 26-33, 1988.

[5] R. Foale et al, "Echocardiographic measurement of the normal adult right ventricle," *Br Heart J*, vol. 56: pp. 33-44, 1986.

[6] S. Malm et al, "Accurate and Reproducible Measurement of Left Ventricular Volume and Ejection Fraction by Contrast Echocardiography: A Comparison with Magnetic Resonance Imaging," *JACC,* vol. 44, no. 5, pp. 1030-1035, Sep. 2004.

[7] W. W. Lai et al, "Guidelines and Standards for Performance of a Pediatric Echocardiogram: A Report from the Task Force of the Pediatric Council of the American Society of Echocardiography," *J Am Soc Echocardiogr*, vol. 19, pp. 1413-1430, 2006.

[8] J. P. McGahan, "Sonography of the Fetal Heart: Findings on the Four-Chamber View," *AJR,* vol. 156, pp. 547-553, Mar. 1991.

[9] E. Tegnander et al, "Incorporating the four-chamber view of the fetal heart into the second-trimester routine fetal examination," *Ultrasound Obstet. Gynecol*., vol. 4, pp. 24-28, 1994.

[10] R. C. Gonzalez et al, "Morphological Image Processing," in *Digital Image Processing Using MATLAB*, Upper Saddle River, NJ: Pearson, 2004, pp. 334-377.

[11] R. C. Gonzalez et al, "Image Segmentation," in *Digital Image Processing Using MATLAB*, Upper Saddle River, NJ: Pearson, 2004, pp. 378-425.

[12] G. Coppini et al, "Recovery of the 3-D Shape of the Left Ventricle from Echocardiographic Images," *IEEE Trans. Med. Imag.*, vol. 14, no. 2, pp. 301-317, Jun. 1995.

[13] J. M. B. Dias and J. M. N. Leitão, "Wall Position and Thickness Estimation from Sequences of Echocardiographic Images," *IEEE Trans. Med. Imag.*, vol. 15, no. 1, pp. 25-38, Feb. 1996.

[14] F. Davignon et al, "Ultrasound data segmentation based on tissue characterization," *Proc. of SPIE,* vol.5750, pp. 447-454, 2005.

[15] The MathWorks, Inc. *Wiener2* [online]. Available: http://www. mathworks.com/help/images/ref/wiener2.html.

[16] D. Lopes. (2007, May 16). *Anisotropic Diffusion (Perona & Malik)* [online]. Available: http://www.mathworks.com/matlabcentral/file exchange/14995-anisotropic-diffusion--perona---malik-.

[17] S. Lankton. (2008, Apr 15). Active Contour Segmentation [online]. Available: http://www.mathworks.com/matlabcentral/fileexchange /19567-active-contour-segmentation.

[18] M. Gaubatz. MetriX MuX Home Page [online]. Available: http:// foulard.ece.cornell.edu /gaubatz/metrix_mux/.

[19] J. Weickert, "Image smoothing and restoration by PDEs," in *Anisotropic Diffusion in Image Processing*, B.G. Teubner Stuttgart, 1998, pp. 1-53.

[20] T. F. Chan and L. A. Vese, "Active Contours Without Edges," IEEE Trans. Image Process., vol. 10, no. 2, pp. 266-277, Feb. 2001.